



UNIVERSIDADE ESTADUAL DE CAMPINAS
SISTEMA DE BIBLIOTECAS DA UNICAMP
REPOSITÓRIO DA PRODUÇÃO CIENTÍFICA E INTELLECTUAL DA UNICAMP

Versão do arquivo anexado / Version of attached file:

Versão do Editor / Published Version

Mais informações no site da editora / Further information on publisher's website:

<https://cdnsiencepub.com/doi/10.1139/cjc-2014-0034>

DOI: 10.1139/cjc-2014-0034

Direitos autorais / Publisher's copyright statement:

©2014 by Canadian Science. All rights reserved.

DIRETORIA DE TRATAMENTO DA INFORMAÇÃO

Cidade Universitária Zeferino Vaz Barão Geraldo

CEP 13083-970 – Campinas SP

Fone: (19) 3521-6493

<http://www.repositorio.unicamp.br>

Deposition of organic–inorganic hybrid coatings over 316L surgical stainless steel and evaluation on vascular cells

F.G. Doro, A.P. Ramos, J.F. Schneider, U.P. Rodrigues-Filho, M.A.M.S. Veiga, C.L. Yano, A. Negreti, M.H. Krieger, and E. Tfouni

Abstract: Surface coating of metallic materials using the sol-gel technique is a suitable approach to obtain hybrid materials with improved properties for biomedical applications. In this study, an AISI 316L stainless steel surface was coated with ormosils prepared from tetraethylsiloxane and 3-glycidoxypropyltrimethoxysilane or polydimethylsiloxane. The characterization of structural and surface properties was performed by several techniques. Surface microstructure, morphology, and energy are dependent on organosilane type and content. Chemical stability of coatings was investigated by static immersion tests in phosphate buffer solution at 37 °C, and silicon leaching after 21 days was found to be in the range of $\sim 200\text{--}300\ \mu\text{g L}^{-1}$. Mechanical adhesion was found to be within 1.0 and 3.7 N cm⁻¹. The interaction of the samples and materials in the cardiovascular environment was investigated through cellular behavior. Biological assays were performed with slides to avoid any cytotoxic effects on human endothelial cells (HUVEC) and rabbit arterial smooth muscle cells (RASM). No significant alterations were observed after 24 h in the viability of RASM and HUVEC cells exposed to different coatings. No increase of HUVEC or RASM migration was observed after 24 h as evaluated by transwell migration assay. The hybrid materials showed suitable properties for potential application as biomaterials in cardiovascular environment as well as for incorporation of bioactive species with the aim to prepare drug-eluting stents.

Key words: ormosil, hybrid coating, biomaterial, sol-gel, stent, vascular cells.

Résumé : Le revêtement de la surface de matériaux métalliques à l'aide du procédé sol-gel est une méthode particulièrement bien adaptée à la fabrication de matériaux hybrides dotés de propriétés améliorées et destinés à des applications biomédicales. Dans la présente étude, la surface d'un acier inoxydable de type AISI 316L a été recouverte d'ormosils produits à partir de tétraéthylsiloxane et de 3-glycidoxypropyltriméthoxysilane ou de polydiméthylsiloxane. La caractérisation des propriétés de structure et de surface a été effectuée suivant plusieurs techniques. La microstructure, morphologie et énergie de surface dépendent des types d'organosilanes utilisés et de leur contenu. La stabilité chimique des revêtements a été analysée au moyen d'essais d'immersion dans une solution tampon de phosphat à 37 °C et du lixiviat de silicium a été détecté après 21 jours à des concentrations d'environ 200 à 300 $\mu\text{g L}^{-1}$. Les mesures d'adhésion mécanique étaient comprises entre 1,0 et 3,7 N cm⁻¹. L'interaction entre les échantillons et les matériaux dans le système cardiovasculaire a été analysée sur le plan du comportement cellulaire. Des essais biologiques ont été réalisés sur des lames pour éviter tous effets cytotoxiques sur les cellules endothéliales humaines (cellules endothéliales veineuses ombilicales humaines) et les cellules musculaires lisses artérielles de lapin. Aucune baisse significative de la viabilité des cellules musculaires lisses et cellules endothéliales exposées à différents revêtements n'a été constatée après 24 h. Par ailleurs, aucune augmentation de la migration de ces deux types de cellules n'a été observée après 24 h selon les résultats des essais de migration transwell. Les matériaux hybrides ont présenté des propriétés compatibles avec leur possible utilisation comme biomatériaux dans le système cardiovasculaire et avec leur association à des espèces bioactives dans le but de fabriquer des stents à élution médicamenteuse. [Traduit par la Rédaction]

Mots-clés : ormosil, revêtement hybride, biomatériau, sol-gel, stent, cellules vasculaires.

Introduction

Different materials such as metals, ceramics, biodegradable or synthetic polymers, composites, or hybrid materials are used in medical devices^{1–4} and invariably come into contact with tissues and body fluids. This contact can be short, such as in the case of catheters or cannulae, or as long as the person's lifetime, as with

bone plates, anchors, and vascular grafts, for example. In all cases, mechanical strength, hardness, and chemical stability, not to mention appropriate biocompatibility, are crucial factors.^{5,6}

AISI 316L surgical stainless steel (SS) is one of the most used alloys in medical devices such as stents.^{7,8} Intravascular stents are medical devices used as a biological scaffold, mostly for diseased arteries, after balloon angioplasty.^{7,9} Compared to angioplasty

Received 23 January 2014. Accepted 29 May 2014.

F.G. Doro. Departamento de Química, Faculdade de Filosofia, Ciências e Letras de Ribeirão Preto. Universidade de São Paulo, 14040-901, Ribeirão Preto, SP, Brazil; Departamento de Química Geral e Inorgânica, Instituto de Química, Universidade Federal da Bahia, 40170-290, Salvador, BA, Brazil.

A.P. Ramos, M.A.M.S. Veiga, and E. Tfouni. Departamento de Química, Faculdade de Filosofia, Ciências e Letras de Ribeirão Preto. Universidade de São Paulo, 14040-901, Ribeirão Preto, SP, Brazil.

J.F. Schneider. Instituto de Física de São Carlos, Universidade de São Paulo, São Carlos, Brazil.

U.P. Rodrigues-Filho. Instituto de Química de São Carlos, Universidade de São Paulo, CP 780, 13563-120 São Carlos, SP, Brazil.

C.L. Yano, A. Negreti, and M.H. Krieger. Departamento de Fisiologia e Biofísica, Instituto de Biologia, Universidade Estadual de Campinas, UNICAMP, SP, Brazil.

Corresponding author: Elia Tfouni (e-mail: eltfouni@usp.br).

This article is part of a Special Issue dedicated to Professor Barry Lever in recognition of his contributions to inorganic chemistry across Canada and beyond.

alone, the stenting procedure improves the safety and efficacy of the intervention, especially by avoiding the abrupt vessel closure. Restenosis remains the main cause of clinical complications even after a stenting procedure, leading to up to 30% failure after 3 months of implantation.^{9,10} In this regard, the use of drug-eluting stents has been shown to be efficient in reduction of in-trastent restenosis.^{11,12} Nonetheless, with the increasing use of drug-eluting stents, other issues, such as stent thrombosis, have emerged.¹² Since restenosis and thrombosis are caused by multiple factors, an ideal stent coating should not only inhibit thrombus formation and proliferation of smooth muscle cells but also facilitate the process of re-endothelialization.^{12,13} Thus, materials for medical devices should minimize the risks from design failure or biological incompatibility. Although the scope of ISO 10993-1 specifically excludes biological risks arising from any mechanical failure, the Food and Drug Administration believes that this potential risk is important to consider when designing biocompatibility studies.¹⁴ For certain devices, such as those that incorporate a coating or multiple material components, it is possible that mechanical failure may change the biological response to the device.^{6,8}

To improve the effectiveness of stents and to overcome the challenges associated with their use, a number of optimization strategies have been employed.¹⁵ Besides those, the biological performance strongly depends on the first interaction when implant surfaces come into contact with a biological environment.^{16,17} For this reason, the control of surface properties, chemical and topographical, is very critical for improving biocompatibility and bio-functionality of implanted materials in a vascular environment.¹⁸ Another factor to consider is the challenge of cell line based screening for “biocompatibility” to connect these cultured cell responses with devices in vitro under controlled conditions for predictions about their behavior in more complex biological systems.^{19,20}

The sol-gel process provides a versatile method to easily prepare organic–inorganic hybrid materials.^{21,22} These hybrid materials, referred to as organically modified silicates (ormosils), are formed by hydrolysis and condensation of organically modified silanes with a common silicon alkoxide or silicon chloride precursor.²³ Organic–inorganic hybrid coatings have been extensively studied in corrosion protection and functionalization of metallic material surfaces including SS.^{24–28} Corrosion leads to undesirable leaching of metal ions from stent grafts that may elicit adverse reactions and decrease the structural integrity of the implants.^{8,29} One viable approach for coating a SS surface is the material sintering (heating from 300 up to 800 °C) following ormosil deposition.^{26,27} While this approach is useful in corrosion protection, it cannot be used for coatings intended to carry bioactive molecules, such as those used in drug-eluting stents. In this case, the approach requires the suitable choice of organosilane that also should afford flexibility and chemical and mechanical stability as well as a way to control the physical properties of resulting ormosils such as permeability.³⁰ The sol-gel process is also an attractive method for application in the biomedical field. Indeed, sol-gel-processed materials have been successfully applied in the development of biocompatible materials,³¹ in the improvement of biocompatibility of currently employed materials,^{32,33} and in the preparation of drug-releasing systems.^{34,35} Since the interaction of cells, such as endothelial cells and platelets, with the surface of the material is influenced by its morphology and chemical composition, the suitable choice of alkoxy and organosilanes sol-gel precursors and processing conditions should constitute an appropriate method to control the materials–cells interaction and cell response. This approach may lead, for instance, to the reduction of platelet adhesion and enhancement of cellular proliferation of endothelial cells on the surface of the material that would contribute to the mitigation of restenosis and thrombus formation.³⁶ The incorpo-

ration of bioactive molecules in a xerogel matrix (bulk or surface) such as NO donors is also possible.³⁷

As part of our ongoing efforts to design NO donor species and materials,^{38,39} we report here the deposition process of organic–inorganic hybrid coatings on 316L SS by the sol-gel technique to be used in the development of drug-eluting stents. The hybrid coatings and resulting materials were prepared using tetraethoxysilane (TEOS) and an organosilane, 3-glycidoxypropyltrimethoxysilane (GLYMO), or polydimethylsiloxane (PDMS) as precursors and characterized with a wide range of techniques. Chemical stability and mechanical adhesion of coatings on SS were also investigated. Biological assays were performed with slides to analyze the biocompatibility of human endothelial cells (HUVEC) and rabbit arterial smooth muscle (RASM) cells by a cytotoxicity assay. The functional aspect was evaluated by a transwell migration assay because this is the major effect to be prevented with this device.

Experimental

Materials

TEOS from Strem Chemicals, GLYMO from Degussa, and silanol-terminated PDMS with an average molecular weight of 2200 g·mol⁻¹ from Dow Corning, ethyl alcohol and isopropyl alcohol from Merck, acetonitrile (ACN) from Aldrich, and hydrochloric acid from J.T Baker were used as received. Dibutyltin dilaurate from Aldrich was used in a 3% (w/w) hexane solution. Stock standard solutions of silicon and tin at a concentration of 1000 mg L⁻¹ for inductively coupled plasma mass spectrometry (ICP-MS) were obtained from Merck. Working standard solutions were obtained by appropriate dilution of stock solutions with phosphate buffer solution (PBS). All other chemicals were reagent grade and used without purification.

Surface treatment of surgical 316L SS

Flat AISI 316L SS slides (10 mm × 10 mm × 1 mm or 20 mm × 20 mm × 1 mm) (Fenix Metais, Brazil) were used as metallic substrates. The surface of slides was sequentially sanded with SiC papers Nos. 1200, 1500, and 2000 (3M) and polished with alumina (0.05 μm) using a polishing cloth (AROTEC) until a mirror-like surface was obtained. Chemical cleaning was performed by dipping slides in NH₄OH–H₂O₂–H₂O (1:1:5 v/v) solution for 10 min, washing extensively with deionized water, dipping in deionized water at 75 °C, and drying under a filtered nitrogen flux. Other cleaning methods were investigated without previous surface polishing but no suitable wettability was achieved (see Supplementary material, Table S1 and Fig. S1).

Preparation and deposition of ormosil coatings

Ormosil coatings were prepared by the sol-gel method using binary mixtures of TEOS/PDMS or TEOS/GLYMO. The TEOS/PDMS sol solutions were obtained by mixing the siloxane and the silane in weight ratio of 90:10 or 70:30 (0.2 or 0.6 g of PDMS, respectively) in 1.5 mL isopropyl alcohol under stirring for 20 min at room temperature in a one-step procedure. ACN (0.5 mL) and dibutyltin dilaurate (three drops) were then added and the mixture was further stirred for 10 min. The resulting sol was left aside for 5 h (or 1 h for 70:30) at room temperature to form a gel. Ormosil coatings obtained as described will be denoted in this work as T₉₀P₁₀ and T₇₀P₃₀, respectively. The TEOS/GLYMO sol solutions were obtained in a two-step procedure using siloxane and silane in a weight ratio of 70:30 or 30:70 (0.3 or 0.7 g of GLYMO, respectively). In solution 1, GLYMO, 0.2 mL of 0.1 mol L⁻¹ HCl solution, and 1.0 mL of ethyl alcohol were mixed under stirring. The addition of acid catalyst to the GLYMO solution is due to the low rate of hydrolysis and condensation of alkylsilanes.⁴⁰ In solution 2, TEOS, 0.5 mL of water, and 1.0 mL of ethyl alcohol were also mixed under stirring. After 40 min, the two solutions were mixed and one drop of perfluoro matrix composite polymer was added to increase solution viscosity. The resulting mixture was further stirred for 30 min and left

aside for 24 h to form a gel. The ormosil coatings obtained with this procedure will be denoted as $T_{70}G_{30}$ and $T_{30}G_{70}$. In all cases, ormosil coatings were deposited on SS slide surfaces by the spin-coating technique. The coatings were allowed to solidify for ~10 min and then dried in an oven at 50 °C for 24 h and stored in a desiccator at room temperature until used.

Ormosil coating characterization

The coating thicknesses were measured by specular reflectance using NanoCalc 2000 equipment (MIKROPACK) with a halogen lamp, optical fiber FCTR-IR400-2-MEFR, and double-channel spectrophotometer 2058 pixel CCD type. The static contact angle of bare SS slides and ormosil-coated SS slides (average of at least three measurements taken with different samples) was determined using a Dataphysics OCA 20 automatic tensiometer, depositing a sessile drop (30 μL) of deionized water on the surface. Surface energy was also determined with the same equipment employing water, *n*-dodecane, and diiodomethane as test liquids. The calculation was made using the Owens-Wendt-Kaelble equation:

$$\gamma_L(1 + \cos \theta) = 2(\gamma_L^d \gamma_S^d)^{1/2} + 2(\gamma_L^p \gamma_S^p)^{1/2}$$

where subscripts S and L represent solid and liquid surfaces, respectively, γ^d represents the dispersion component of the total surface energy (γ), and γ^p is the polar component.⁴¹ Scanning electron microscopy (SEM) was recorded on a Zeiss EVO 50 equipped with an EDS detector. Atomic force microscopy (AFM) was carried out on a Shimadzu SPM 9600 model using the tapping mode (TM). Images were processed with Gwyddion version 2.31 or SPIP (scanning probe image processor) version 6.0.2 (Denmark). The topographic and phase images were recorded simultaneously using a standard silicon tip with radius of 6 nm. The scan rate used was 0.5 or 1.0 Hz. Determination of surface roughness values was done by root mean square for GLYMO-containing coatings on an area of 50 \times 50 μm^2 . Root mean square values were calculated using SPIP version 6.0.2.

High-resolution solid-state NMR and vibrational spectroscopy

Samples of the organic-inorganic hybrid materials (~1.0 g) for NMR experiments were obtained by the same procedure described above except that gel was spread on a Teflon plate, carefully removed after drying, and then ground to a powder. ¹³C and ²⁹Si solid-state high-resolution NMR spectra were obtained on a Varian Unity INOVA 400 (9.4 Tesla) spectrometer and a 7 mm Varian-Jakobsen probe. The magic angle spinning (MAS) technique was used with a spinning frequency of 7 kHz. ²⁹Si NMR spectra were measured by direct polarization applying a single radio frequency $\pi/2$ pulse of 4.0 μs . A recycle time of 300 s was sufficient to ensure complete magnetization recovery of all silicon species. For the ¹³C spectra, the direct polarization measurements were obtained from single-pulse experiments with a $\pi/2$ pulse of 4.0 μs and a recycle time of 5 s. The nonquaternary-suppressed (NQS) experiment was conducted to determine which lines corresponded to a carbon with a strong ¹H-¹³C dipolar magnetic interaction. Time intervals between pulse and decoupling were 100 μs . For ¹H-¹³C cross-polarization (CP) experiments, a $\pi/2$ ¹H pulse of 3.5 μs was applied with a contact time of 1 ms and a recycle delay of 3 s. The high-power ¹H decoupling technique was applied during acquisition to minimize the effect of the ¹H-¹³C dipolar interaction. Solid samples of adamantane and kaolinite were used as secondary standards for ¹³C and ²⁹Si chemical shifts, respectively.

Specular reflectance Fourier transform infrared spectroscopy (FTIR) in the range of 4000–400 cm^{-1} was carried out directly on the surface of ormosil-coated SS slides in a MB-102 Bomem spectrophotometer equipped with a SPECAC Linear Polarizer GS12000

model accessory. IR spectra were also recorded using powdered material dispersed in KBr pellets using the transmittance mode. Very similar spectra pattern were obtained with both techniques.

Mechanical adhesion and chemical stability of the ormosil coatings

Mechanical adhesion was investigated by a peel strength adhesion test in Instron equipment according to ASTM D 1000⁴² using 20 mm \times 20 mm ormosil-coated SS slides at the laboratory of the 3M Brasil production plant at Ribeirão Preto, SP. Adhesion strengths are reported as an average of two tests. Chemical stability of coatings was investigated through static immersion tests. Bare SS slides and those coated with ormosils (10 mm \times 10 mm) were placed in 10 mL of PBS (20 mmol L^{-1} , $\mu = 137$ mmol L^{-1} NaCl, pH 7.4) and incubated at 37 °C. After 7 days, slides were transferred to fresh PBS solutions. This procedure was repeated for up to 21 days to complete. Silicon (²⁸Si) and tin (¹²⁰Sn) concentrations in the soaked solutions were determined using an ICP-MS (Perkin Elmer Scix Elan DRC II). Appropriate dilutions of soaked solutions were performed. The instrument was calibrated with 0–200 $\mu\text{g L}^{-1}$ standard analytes solutions in PBS. Linear coefficients for calibration curves were better than 0.9999. Three samples of each material were used and five runs were performed for each sample.

Biological assays

Cell cultures

RASM cells from a previously established selection-immortalized line^{43,44} were generously supplied by Dr. Helena Nader from the Biochemistry Department of the Federal University of São Paulo (São Paulo, SP, Brazil) and HUVEC were purchased from Invitrogen Life Technologies, USA. Cells were routinely grown in F-12 supplemented with 10% fetal bovine serum, 100 U mL^{-1} penicillin, and 10 mg mL^{-1} streptomycin and in M200 supplemented with 1 $\mu\text{g mL}^{-1}$ hydrocortisone, 10 ng mL^{-1} human epidermal growth factor, 10 ng mL^{-1} heparin, 3 ng mL^{-1} basic fibroblast growth factor, gentamicin–amphotericin, and 20% fetal bovine serum and grown in a 5% CO_2 humidified incubator at 37 °C. The control was untreated cells incubated only with culture medium.

Cytotoxicity assay

Sample cytotoxicity was assessed using the 3-(4,5-dimethylthiazol-2-yl)-2,5-diphenyltetrazolium bromide (MTT) reduction method described by Mosmann.⁴⁵ MTT is converted to blue formazan crystals in mitochondria by dehydrogenase enzymes of viable cells. Cells were seeded on a 12-well plate (1×10^6 cells) and were exposed to bare SS slides and $T_{70}P_{30}$ and $T_{30}G_{70}$ ormosil-coated slides for 24 h and compared to the control without materials. After incubation for 4 h with 5×10^{-3} g mL^{-1} MTT solution at 37 °C, absorbance was determined at 570 nm using an ELISA reader (Bio-Tek Instruments, Inc., USA). Each test was repeated at least three times with controls in each microplate included. Each value of the different samples and controls was based on the mean of five to eight wells and the standard error of the mean was calculated based on values obtained by these independent experiments.

Transwell migration assay

Cell migration assays were carried out using a BioCoat 24-multiwell insert system (BD Biosciences) with an 8 μm pore size polycarbonate filter insert that divides the chamber into upper and lower portions. HUVEC and RASM cells were cultured in bottles until confluence and serum deprived overnight. After this period, the cells were trypsinized and resuspended in M200 medium (GIBCO) containing 0.5% fetal calf serum. Density of 1×10^5 cells per well were added to the top of the insert in a final volume of 200 μL of M200 medium (GIBCO). Fetal calf serum at 10% and 20% was used for the stimulus of migration on the HUVEC and RASM cells during a period of 24 h, respectively. In the ab-

sence or presence of slides, MTT was added and cells were incubated for an additional period of 4 h. Cells from the top of the transwell chambers were removed using a cotton swab (residual cells). The transwell chamber (migrated) cells were placed in separate wells of a 24-well plate containing 400 μL of dimethylsulfoxide. Following 1 h of gentle shaking, 100 μL samples were removed for 96-well plate and absorbance was determined at 570 nm using an ELISA plate reader.

Results and discussion

Ormosil coating preparation and characterization

Since the surface homogeneity and hydrophilicity of a metallic substrate largely influence the adhesion and morphology of coated thin films,⁴⁶ the SS slides were polished and cleaned prior to film deposition. The method used in this work increased the wettability of the SS surface as evidenced by the reduction in the water static contact angle (θ_{water}). The values of $\theta_{\text{water}} = 83^\circ \pm 3^\circ$ and $\theta_{\text{water}} = 41^\circ \pm 2^\circ$ were found for the untreated and polished and cleaned SS slides, respectively. The wettability obtained after surface polishing and cleaning was better than that obtained using chromic acid as a cleaning agent ($\theta = 69^\circ \pm 7.2^\circ$)⁴⁷ but poorer than that obtained with polishing and air plasma cleaning ($\theta = 22^\circ \pm 2^\circ$).⁴⁸ Nonetheless, the obtained degree of surface hydrophilicity was suitable for thin film deposition.

The ormosil-coated SS slides were prepared by the sol-gel method and characterized by a multitechnique approach to investigate properties such as the structure of the xerogel network, microstructure, nanostructure, mechanical adhesion, and chemical stability. Since one of the goals of this work is to develop ormosils to coat stent surfaces with potential application in NO-eluting stents by doping the thin films with NO donors, organosilanes were carefully chosen. PDMS or GLYMO is expected to improve the viscoelasticity of the resulting ormosils, leading to a suitable mechanical rigidity to resist torsional forces, since the stent can undergo compression and expansion in the vascular environment. Addition of GLYMO into hybrid organic-inorganic coatings has been reported to improve mechanical resistance and adhesion.⁴⁹ Ormosils containing PDMS can reduce platelet adhesion.⁵⁰ This alkylsilane also shows a high gas permeability, which is important for the desired application.

It is worth mentioning that other several sol-gel processing conditions such as the TEOS to organosilane ratio, solvent, gelation time, and condensation catalyst were investigated. None of these resulted in coatings with a homogeneous and crack-free surface and (or) suitable adhesion to SS. Among the optimized conditions, we choose a high and low GLYMO to TEOS ratio to evaluate their effect on the ormosil properties. To compare GLYMO and PDMS as additives for coatings, a similar rationale was followed.

The thicknesses of coatings were measured by specular reflectance. The coating thicknesses highly depend on rheological, formulation, and processing parameters. Since these features changed significantly for the ormosil preparations, the thicknesses for PDMS materials, $T_{70}P_{30}$ ($3.74 \pm 0.08 \mu\text{m}$) and $T_{90}P_{10}$ ($0.97 \pm 0.06 \mu\text{m}$), showed values different from those obtained for GLYMO, $T_{30}G_{70}$ ($2.21 \pm 0.04 \mu\text{m}$) and $T_{70}G_{30}$ ($1.50 \pm 0.02 \mu\text{m}$).

Characterization of structural properties of ormosils

Specular reflectance FTIR and NMR techniques were used to investigate the network formation and structural properties of ormosil coatings. FTIR spectra for $T_{70}P_{30}$ and $T_{30}G_{70}$ coatings on SS slides are given in the supplementary material (Fig. S2).

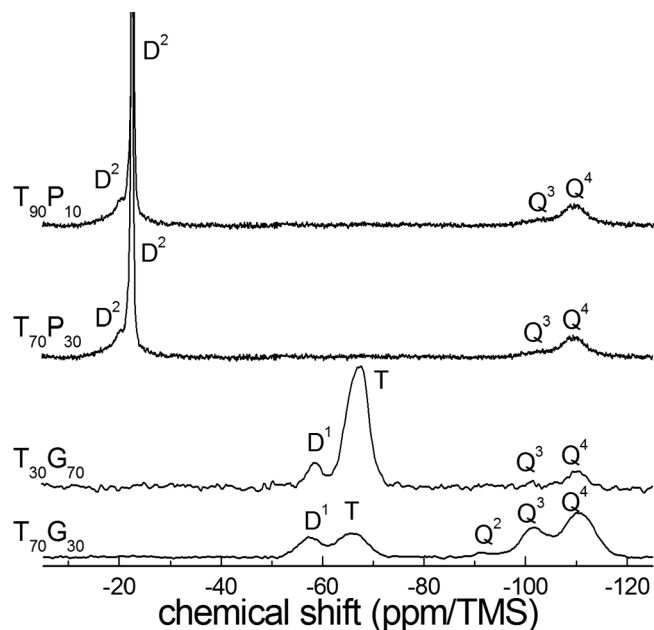
The FTIR spectrum of the $T_{70}P_{30}$ ormosil coating presents the main characteristic absorption bands of PDMS. The bands associated with methyl groups of symmetric stretching ($\nu_s\text{CH}_3$), asymmetric stretching ($\nu_{as}\text{CH}_3$), and symmetric deformation vibrations (δCH_3) appear at 2960, 2908, and 1260 cm^{-1} , respectively.⁵¹ For the lower energy region of the spectrum (1200–700 cm^{-1}), the assign-

ment is not so straightforward. Polysiloxanes show vibration modes associated with Si–O–Si. The antisymmetric stretching ($\nu_{as}\text{SiO}$) occurs near 1050 cm^{-1} in PDMS⁵² and thus, $\nu_{as}\text{SiO}$ is probably related to the 1040 cm^{-1} band observed in the $T_{70}P_{30}$ spectrum. However, the antisymmetric band may be regarded as a superposition of two bands, one corresponding to the $\nu_{as}\text{SiO}$ vibration of two siloxane neighbors and the other to their antisymmetric motion.⁵² This band in PDMS was found to split into two components. In our spectrum, this major band is split into two components, 1050 and 1010 cm^{-1} . It should be pointed out that the $\nu_{as}\text{SiO}$ of Si–O–Si groups (1100–1000 cm^{-1} region) is also related to the extent of the in situ condensation reaction of the TEOS hydrolysis product. Indeed, Q^3 and Q^4 species are detected in the ²⁹Si NMR spectra (see below). The symmetric stretching of Si–O–Si ($\nu_s\text{SiO}$) in PDMS has an IR absorbance below 900 cm^{-1} near the range of the νSiC and ρCH_3 bands. Since CH_3 rocking and Si–C stretching modes appear in the region ~ 870 –750 cm^{-1} , it is reasonable to assume that the two peaks in this region (850 and 790 cm^{-1}) correspond to these modes. The presence of a band at 850 cm^{-1} in TEOS/polysiloxane-based materials has been proposed to arise from condensation between TEOS and PDMS molecules during gel formation.⁵³ A similar pattern was observed in the FTIR spectrum of $T_{90}P_{10}$.

The FTIR spectrum of the $T_{30}G_{70}$ ormosil coating on SS slide surfaces (Fig. S2) is dominated by a strong two-component band due to $\nu_s\text{SiO}$ stretching modes near 1100 cm^{-1} . Weak intensity absorption bands at 2980 and 2870 cm^{-1} can be assigned to $\nu_s\text{CH}$ and $\nu_{as}\text{CH}$ stretching modes of the methylene groups of GLYMO.⁵⁴ The broad band of hydroxyl groups near 3400 cm^{-1} is due to either entrapped water remaining after film drying or, more likely, silanol (Si–OH) groups formed by the hydrolysis of alcoxysilanes. It is known that the epoxy ring of GLYMO can undergo an opening reaction depending on the sol-gel processing conditions.⁵⁵ The epoxy rings have characteristic IR bands at 1260–1240 cm^{-1} (ring breathing) and 950–810 cm^{-1} (ν_{as} ring stretching) regions.⁵⁴ For $T_{30}G_{70}$, these bands can be found at 1255 and 908 cm^{-1} in FTIR. These results indicate that epoxy rings do not undergo hydrolysis to a significant extent. The preservation of these groups can be of particular interest, since oxirane ring opening results in diol and oligo(ethylene glycol) groups.⁵⁶ These groups could increase the surface energy contributing to an undesired increase in adhesion of platelets. The FTIR spectrum of $T_{70}G_{30}$ also showed the characteristic bands of GLYMO with no major differences compared to $T_{30}G_{70}$, except those expected as the result of an increase in TEOS content. For instance, more intense bands near 3400 cm^{-1} and at 940 cm^{-1} were observed for $T_{70}G_{30}$ probably due to a higher content of silanol (Si–OH) groups (see below).

High-resolution solid-state ²⁹Si NMR spectra, shown in Fig. 1, were obtained for PDMS and GLYMO organic-inorganic hybrid materials. The ²⁹Si NMR resonances were attributed to silicon species according to their chemical shifts.^{57,58} These species are identified with the notation D^2 $\{(\text{C})_2\text{Si}(\text{OSi})\}$, D^1 $\{\text{CSi}(\text{OSi})_2(\text{OH})\}$, T $\{\text{CSi}(\text{OSi})_3\}$, and Q^n $\{\text{Si}(\text{OSi})_n(\text{OH})_{4-n}\}$, where n denotes the number of siloxane bonds established by the probed silicon atom. Table 1 shows the populations of silicon species obtained from the integrated intensities of the ²⁹Si NMR lines.

The ²⁹Si MAS NMR spectra of the ormosils containing PDMS ($T_{90}P_{10}$ and $T_{70}P_{30}$) (Fig. 1) are dominated by a peak centered at -22 ppm that can be attributed to D^2 species of PDMS molecules.⁵⁹ The narrowness of this resonance (0.3 ppm in $T_{90}P_{10}$ and 0.8 ppm in $T_{70}P_{30}$) indicates high molecular mobility for these silicon groups. There are two additional resonances at -19.7 and -21.5 ppm, both weaker and broader than the main one, corresponding also to D^2 silicon species with low mobility, as usually observed in solid phases. There are resonances at -102 and -109.5 ppm, which can be respectively attributed to Q^3 and Q^4 silicon resulting from the hydrolysis of TEOS. These results suggest the presence of free liquid-like PDMS and partially grafted PDMS on a silicate network

Fig. 1. Single-pulse ^{29}Si MAS NMR spectra of ormosils.**Table 1.** Relative intensities (%) of ^{29}Si NMR lines.

Ormosil	D ²	D ²	D ²	D ¹	T	Q ²	Q ³	Q ⁴
T ₉₀ P ₁₀	13	13	36				14	24
T ₇₀ P ₃₀	1	7	75				3	14
T ₇₀ G ₃₀				13	21	3	22	41
T ₃₀ G ₇₀				11	79		1	9

formed by TEOS hydrolysis. Table 1 shows a decrease of Qⁿ sites from T₉₀P₁₀ to T₇₀P₃₀ with a concomitant increase of D² sites, which is consistent with the increase in the PDMS to TEOS ratio.

The ^{29}Si NMR spectra of GLYMO-containing ormosils, T₃₀G₇₀ and T₇₀G₃₀ (Fig. 1), show signals from D¹ (−58 ppm) and T (−67 ppm) in addition to the Qⁿ species. The results on Table 1 show that T₇₀G₃₀ has the highest fraction of Qⁿ species, i.e., the highest concentration of condensed silicates. The higher population of T silicon sites is observed in T₃₀G₇₀, the sample with the highest content of GLYMO, indicating the occurrence of self-condensation. It should be noted that the fractions of D¹ and Q³ sites in T₇₀G₃₀ are higher than those in T₃₀G₇₀ and even Q² sites are present. Since such sites present residual silanol groups, they contribute to a more intense absorption band centered at 3400 cm^{−1} as observed in FTIR for T₃₀G₇₀. Figure 2 shows the ^{13}C NMR spectra obtained with direct polarization, $\{^1\text{H}\}$ -CP, and NQS techniques in GLYMO-containing ormosils.

The ^{13}C NMR spectra of T₃₀G₇₀ in Fig. 2 shows a set of six intense and well-defined signals that can be readily attributed to the organic chain of GLYMO, according to the scheme in the figure.⁶⁰ The same set of signals is present in the spectrum of T₇₀G₃₀. The comparison of the CP spectra shows that the resonances in T₇₀G₃₀ are considerably broadened compared to those observed in T₃₀G₇₀. This difference indicates reduced mobility of alkyl groups and (or) the presence of different chemical environments in T₇₀G₃₀. In the sample T₇₀G₃₀, the spectral region corresponding to the C–O bonds, above 70 ppm, shows a multiplicity of sites. The intensity of these resonances is different in the DC, CP, and NQS spectra, indicating differences in their dipolar coupling with ^1H . The narrow lines observed in the NQS spectrum indicate low dipolar coupling with ^1H , as the C₃ and C₄ resonances observed in the sample T₃₀G₇₀. This multiplicity might be attributed in part to the opening of some epoxy rings, by reaction with other rings,

giving rise to poly(ethylene)oxide.⁶⁰ Other possibilities for the reaction of these rings may explain the weaker resonances observed at 64 and 60 ppm, corresponding respectively to methyl-ether and diol carbons. According to the low intensity of these resonances, these reactions are less probable than the mutual polymerization of GLYMO groups. The strong intensity of the epoxy carbons C₅ and C₆ in the direct polarization spectrum indicates a high fraction of integral rings, as observed previously by FTIR. A marginal fraction of ring opening products in T₃₀G₇₀ might be inferred from the detection of a pair of very weak resonances at 59 and 65 ppm, constituting less than 1% of all of the observed carbon.

Coating microstructure, morphology, and surface energy

Since the morphology and chemical composition of the thin films surface affect parameters such as the surface energy and influence on the interaction with biological organelles, like platelets and smooth muscle cells, the morphological features were investigated by means of SEM and AFM. The chemical composition of coatings was studied by static contact angle and surface energy analysis.

According to SEM images, all coatings showed a smooth, homogenous, and crack-free surface (see supplementary Fig. S3). On increasing magnification (from 500× to 5000×), the micrographs of T₃₀G₇₀ showed a surface with homogeneously distributed pores with almost regular sizes (Fig. S3D and S3F). The presence of few pores was detected on the T₇₀G₃₀ surface only by AFM (see below). These results suggest that surface porosity is influenced by the GLYMO to TEOS ratio. The PDMS materials did not show the presence of pores on the surfaces according to SEM.

The microstructure and morphology of ormosil coatings on SS slides were investigated by TM-AFM. Representative AFM images for T₉₀P₁₀ and T₃₀G₇₀ are shown in Fig. 3.

Figure 3 shows that ormosil coatings containing PDMS or GLYMO have quite different morphology. The T₉₀P₁₀ coating showed several spots on topographic images that are also seen in phase contrast. Since the contrast in phase images with different viscoelasticity is different, such a difference in viscoelasticity was tentatively assigned to segregation of free PDMS and siliceous-rich domains.⁶¹ The formation of these domains was rationalized as a consequence of diffusion of nonnetwork species to the surface.⁶¹ Indeed, the positive shift of the cantilever observed in TM-AFM as the tip senses the stiffer siliceous-rich domain would result in lighter images, as observed (Fig. 3B). Similarly, the darker images would be the result of soft PDMS-rich domains. The presence of loosely bound PDMS molecules agrees with the mobile D² species of PDMS molecules observed in ^{29}Si MAS NMR spectra. Similar morphology was observed for T₇₀P₃₀ but with an increase in domain size, suggesting more pronounced phase separation. The TM-AFM analysis (Fig. 3) shows different film morphology for GLYMO-containing ormosils. T₃₀G₇₀ shows homogeneously distributed micrometre-size pores in agreement with SEM images, with pores diameters within the range of 1–4 μm and an average of 2 ± 1 μm. The surface porosity is around 12%. For T₇₀G₃₀, which has a higher TEOS content, a drastic reduction of porosity to less than 1% was found (data not shown). As anticipated in SEM analysis, the TEOS to GLYMO ratio strongly influences the surface porosity. No phase separation for GLYMO-containing ormosils was evident even when higher resolution images (1 × 1 μm²) were recorded.

Along with the surface morphology of coatings, their physico-chemical properties such as hydrophilicity and reactivity are important in the interaction with biological organelles.^{20,62} To get a better comprehension of such parameters, data of water static contact angle and surface energy were collected and are shown in Table 2.

From Table 2, it is possible to observe that the organosilane present on the coating composition has a marked influence on the

Fig. 2. ^{13}C MAS NMR spectra of GLYMO-containing ormosils: (A) $\text{T}_{30}\text{G}_{70}$ and (B) $\text{T}_{70}\text{G}_{30}$. DP, direct polarization single-pulse experiment; CP, $\{^1\text{H}\}$ - ^{13}C cross-polarization experiment; NQS, nonquaternary suppression experiment.

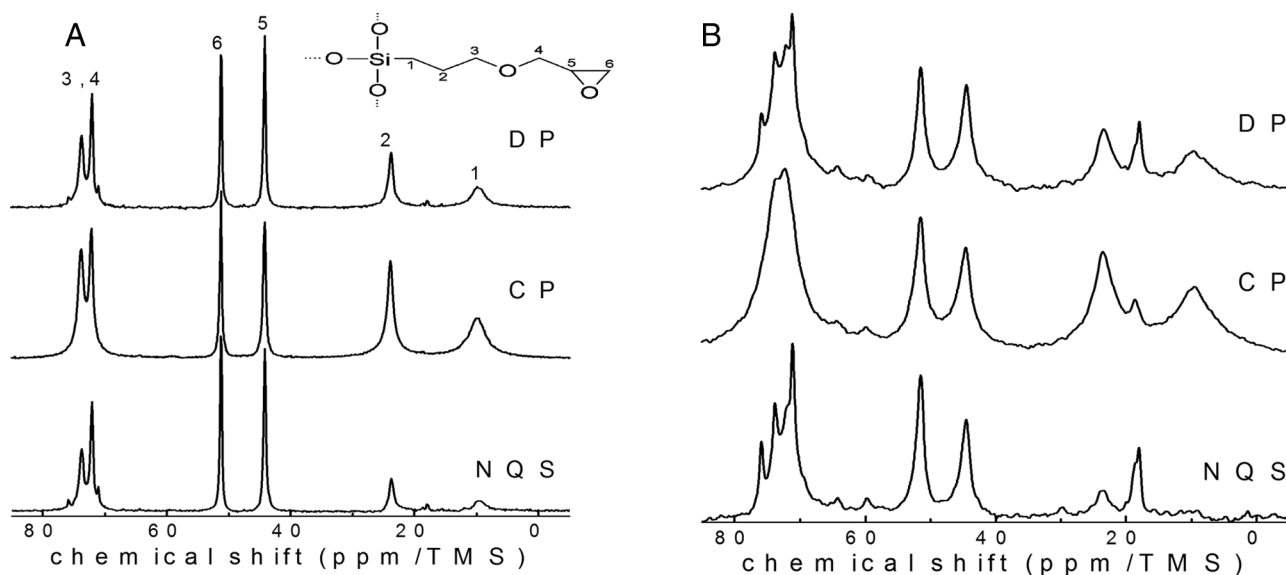


Fig. 3. Representative TM-AFM images of ormosil coatings: (A) topographic, (B) phase-contrast, and (C) 3D view for $\text{T}_{90}\text{P}_{10}$ and (D) topographic, (E) phase-contrast, and (F) 3D view for $\text{T}_{30}\text{G}_{70}$.

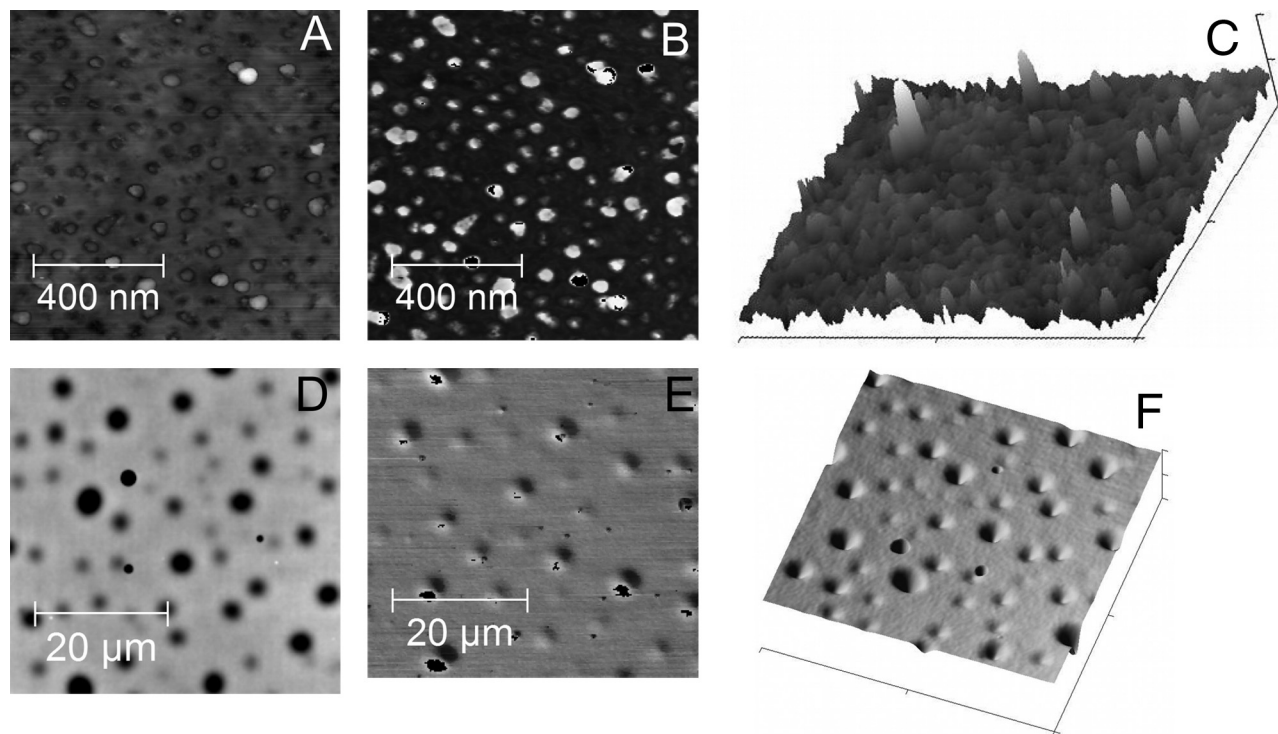


Table 2. Static water contact angle (θ_{water}) and surface energy data of ormosil coatings on a SS surface.

Sample	θ_{water} (°)	Surface energy (mJ m^{-2})
SS	41±3	42.9±2.0
$\text{T}_{90}\text{P}_{10}$	100±2	26.1±2.0
$\text{T}_{70}\text{P}_{30}$	101±2	22.9±1.6
$\text{T}_{70}\text{G}_{30}$	77±3	33.7±2.7
$\text{T}_{30}\text{G}_{70}$	22±4	68.4±5.0

water contact angle and surface energy. In general, using PDMS as precursor, an increase in water contact angle and a concomitant decrease in energy surface compared to bare SS slides were observed. This result was expected considering the structure, chemical composition, and molecular weight of PDMS: its alkyl groups present at the film surface contribute to a decrease in the wettability, which in turn reflects in the higher values of water contact angle and consequently lower energy surface, as observed.⁶³ It is known that ormosil produced with alkyl functional silanes can render superhydrophobic surfaces⁶⁴ that can be turned into superhydrophilic ones depending on calcination conditions. The

Table 3. Silicon leaching and adhesion strength of ormosil coatings.

Sample	Silicon leaching content ($\mu\text{g L}^{-1}$) ^a				Adhesion strength (N cm^{-1}) ^b
	1–7 days	7–14 days	14–21 days	Total 21 days	
T ₉₀ P ₁₀	99±22	93±17	120±14	312±31	2.61±0.5
T ₇₀ P ₃₀	50±14	97±22	48±18	195±32	2.22±0.4
T ₇₀ G ₃₀	102±19	92±19	61±20	255±33	0.99±0.2
T ₃₀ G ₇₀	101±18	59±15	40±12	200±26	3.70±0.5

^aCalculated from silicon ICP-MS results in soak solutions.

^bObtained from 180° peel adhesion test according to ASTM D 1000.⁴²

surfaces produced with our methodology are far from being superhydrophobic, but the low surface energy observed for PDMS-containing ormosils could contribute to decreased platelet adhesion.⁵⁰ For GLYMO-containing ormosils, an antagonistic behavior was detected and the water wettability of the coated surfaces shows a dependence on the TEOS to GLYMO ratio used. For T₇₀G₃₀ coatings, a decrease in the surface energy is observed compared to the bare SS sample. Considering the surface chemistry, this result was expected owing to the hydrophobic feature of the organosilane chemical structure and that only a small fraction of epoxy rings underwent opening reactions, as observed in the ¹³C NMR spectra of T₃₀G₇₀. Upon an increase in GLYMO content as in T₃₀G₇₀, a decrease in water wettability and surface energy should be expected when compared to T₇₀G₃₀ and bare SS. Nevertheless, for T₃₀G₇₀, a decrease in the water contact angle and an increase in the surface energy are observed. Since the contact angle depends on both the chemical composition and the surface roughness at the micrometre level,⁶⁵ these results could be mainly related to the presence of a high quantity of pores in the T₃₀G₇₀ sample. As observed by TM-AFM, T₃₀G₇₀ films showed micrometre-size pores covering around 12% of their surface, while for T₇₀G₃₀, less than 1% was found. Depending on the biological target, the surface porosity and chemistry may be important for migration, as reported by Steele and co-workers on the migration of epithelial tissue in porous polymeric matrices.⁶⁶ The effects of the 0.1 μm diameter pores and the surface hydrophilicity were additive, with the maximal level of epithelial tissue migration occurring on a porous, hydrophilic polymer surface.⁶⁶ The T₇₀G₃₀ and T₃₀G₇₀ films obtained have different porosities, very low porosity for the former and larger for the latter, with one order of magnitude larger pores ($\sim 2 \mu\text{m}$) that may influence the interactions with the biological target.

Mechanical adhesion and chemical stability of ormosil coatings

Despite the biocompatibility of some ormosils, chemical and mechanical stability are crucial factors for biomaterials. Greater stability may provide a longer lifespan for the material and prevent potential undesirable effects associated with release of film components. To investigate if ormosil coatings have suitable mechanical properties and if leaching are occurring, peel adhesion tests and static immersion tests in PBS at 37 °C were performed. ²⁸Si concentration in soak solutions was determined by ICP-MS and was taken as a probe of film component leaching and stability. Since tin catalyst (dibutyltin dilaurate) was used in PDMS-containing ormosils, ¹²⁰Sn presence was also analyzed. Table 3 collects values of silicon leaching and adhesion strength for ormosil coatings.

As show in Table 3, for GLYMO-containing coatings, silicon leaching is higher in the first 7 days possibly due to loss of non-network or weakly attached silicon species and the chemical stability is T₃₀G₇₀ > T₇₀G₃₀ based on the total silicon content in the soak solutions used. Interestingly, for T₇₀G₃₀ and T₃₀G₇₀, the population of silanol-containing species in ormosils seems to influence this parameter. According to ²⁹Si MAS NMR (Table 1), the ratio of D¹ + Q² + Q³/T + Q⁴ is equal to 0.61 for T₇₀G₃₀, while this

value is only 0.25 for T₃₀G₇₀. Dissolution of solid silica in contact with aqueous solution results in monosilicic acid (Si(OH)₄),⁶⁷ or in our case, probably low molecular weight oligosiloxanes, both by depolymerization through hydrolysis of Si–O–Si bonds. Thus, a higher fraction of T and Q⁴ species would restrain the dissolution. For T₉₀P₁₀ and T₇₀P₃₀, the chemical stability is T₇₀P₃₀ > T₉₀P₁₀, which also seems to correlate with the population of silanol-containing species. No detectable increase in ¹²⁰Sn concentration was found in soak solutions for these materials. Although all studied ormosil coatings released some amount of their components, SEM images for T₇₀P₃₀ and T₃₀G₇₀ after 21 days of immersion (data not shown) did not show film detaching or cavitation roles. As will be shown in biological assays, no decrease in viability was observed for the cell lines studied.

According to the peel strength adhesion tests, T₉₀P₁₀ and T₇₀P₃₀ show roughly the same adhesion strength, indicating that interaction of the material with the SS surface is nearly the same and it is not significantly influenced by the TEOS to PDMS ratio investigated in this work. On the other hand, the adhesion strength for T₃₀G₇₀ and T₇₀G₃₀ is very different. Since GLYMO is known to increase the adhesion properties of hybrid materials,⁴⁹ the greater adhesion is probably due to its higher concentration in sol solutions. The adhesion strengths found for our coatings are similar to those obtained with *n*-butyltrimetoxysilane or benzyltrimetoxysilane xerogels coated on a steel surface.⁶⁸ Thus, except for T₇₀G₃₀, all films presented suitable adhesion to SS. Since chemical stability and mechanical adhesion are crucial factors for material performance, biological assays were carried out with T₇₀P₃₀ and T₃₀G₇₀ ormosil coatings.

Vascular cell viability assay

The features of the biomaterial surface are an important prerequisite for the success of several biomedical devices. Routes of biological exposure as well as material chemical and physical properties must be carefully considered in these biocompatibility tests. The cell viability assays determine an insult to the cell to a variable degree and are often used as a general criterion for assessing biocompatibility.⁶⁹ The MTT assay was used for the biocompatibility tests on the two major vascular cellular types. No significant alterations were observed in the viability of RASM cells and HUVEC exposed to different slides (Fig. 4). Thus, bare SS slides and T₃₀G₇₀- and T₇₀P₃₀-coated SS slides showed near 100% biocompatibility.

The results represent an important factor to separate slide-induced artifacts as leaching and cracking of the ormosil coating on the SS surface. In the culture condition, despite the small silicon leaching observed for T₇₀P₃₀ and T₃₀G₇₀ in static immersion tests in PBS at 37 °C (Table 3), no alteration was observed in the behavior of both cell lines. This result may be due to a lack of leaching of silicon species during the time interval and under the physiological conditions of the assays or the amount leached was not sufficient to interfere with the cellular signaling pathways. Indeed, higher concentrations of siliceous compounds seem to be necessary to interfere with HUVEC behavior as observed in the presence of 100 mg L⁻¹ silica nanoparticles, which were able to decrease the cell viability by 28% after 24 h.⁷⁰

Fig. 4. Cell viability of (A) RASM cells and (B) HUVEC exposed to bare SS slides and $T_{30}G_{70}$ - and $T_{70}P_{30}$ -coated SS slides compared to the control after 24 h assessed using the MTT reduction. The results obtained were expressed as a fraction of viable cells and normalized to that of cells without slides (control). The reported data are average values and error bars indicate standard error of the mean of three independent experiments ($p < 0.05$).

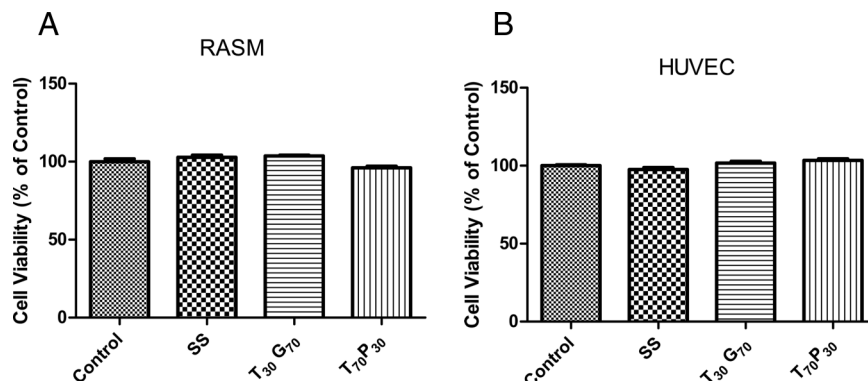
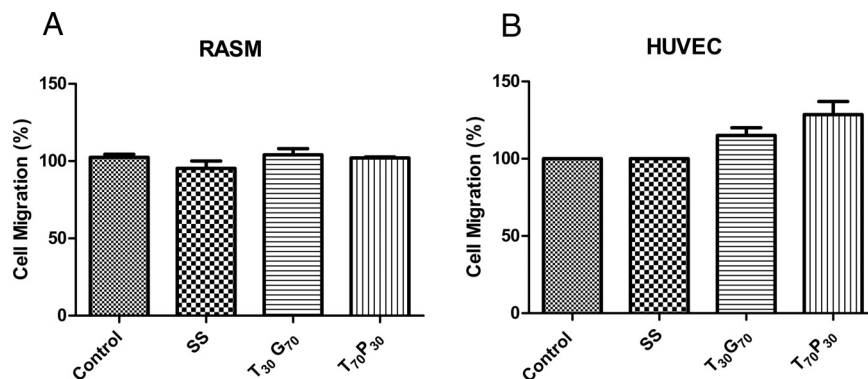


Fig. 5. Cells that migrated onto the lower surface of the membrane through stimulus with fetal calf serum were fixed and stained, as described in Experimental section: (A) RASM and (B) HUVEC migrated cells after a 24 h incubation with bare SS slides and $T_{70}G_{30}$ - and $T_{70}P_{30}$ -coated on SS slides compared to the control. Each point represents the average value and error bars indicate standard error of the mean of triplicate determinations.



Migration assay

The movement of cell migration can be oriented by chemical, physical, and other stimuli and it occurs in a variable sense.⁷¹ The transwell migration assay, adopted here as a functional index, provides a model of vertical direction and it was oriented by stimulus of fetal calf serum. No significant alterations were observed in the migration behavior of RASM cells and HUVEC in the presence of bare SS slides and $T_{70}P_{30}$ and $T_{30}G_{70}$ coatings compared to the control treatment without SS slides after 24 h (Fig. 5). Thus, the presence of bare SS slides and $T_{30}G_{70}$ - and $T_{70}P_{30}$ -coated SS slides does not induce functional alterations.

Conclusions

We have obtained different hybrid materials by coating the surface of AISI 316L SS using the sol-gel technique. Structural data obtained from FTIR and high-resolution solid-state NMR showed differences in the degree of condensation of silicon sites. Higher condensation seems to result in better adhesion strength and chemical stability for TEOS/GLYMO coatings. For TEOS/PDMS coatings, just a small increase in adhesion was observed with an increasing in the degree of condensation of silicon sites. The type and ratio of organosilane also showed influence in the morphology and energy surface of coatings. TEOS/GLYMO ormosils showed microporosity that decreased with increasing TEOS content, which in turn resulted in lower wettability and energy surface. For TEOS/PDMS, microphase separation was observed while low-energy surface coatings resulted. Biocompatibility of the new hybrid materials was investigated with the use of vascular cell lines,

HUVEC and RASM cells. No alteration of cellular viability from both cell lines was observed upon exposure of the materials according to MTT assays. Additionally, no biofunctionality change was observed through migration assays for HUVEC and RASM cells with those coatings tested. Considering the wide range of characterization studies, coating features, and biological responses, $T_{70}P_{30}$ and $T_{30}G_{70}$ coatings are those with suitable properties for vascular applications. Thus, these hybrid materials can be used further for the incorporation of bioactive species with the aim to prepare drug-eluting stents. Preparation of ormosil coatings containing metal nitrosyl complexes as NO donors and their evaluation on vascular cell lines with the aim of developing NO eluting stents are one of our interests and such materials are under current investigation. Safety, efficacy, and durability are properties that are essential for the improvement of drug-eluting stents. The optimal combination of these factors is crucial for the overall performance of the stent and will determine its success among the growing number of alternatives in the field. The hybrid materials described here are promising in this regard.

Supplementary material

Supplementary material for this paper is available on the journal web site at <http://nrcresearchpress.com/doi/suppl/10.1139/cjc-2014-0034>.

Acknowledgements

The authors thank grants and fellowships from São Paulo Research Foundation (FAPESP), Conselho Nacional de Desen-

volvimento Científico e Tecnológico (CNPq), Coordenadoria de Aperfeiçoamentos do Pessoal do Ensino Superior (CAPES), and Fundação de Amparo à Pesquisa do Estado da Bahia (FAPESB) as follows. E. Tfouni: FAPESP grant 2006/53266-4 and CNPq fellowship 308123/2009-3; F.G. Doro: FAPESP fellowship 2003/09578-3 and FAPESB grant PPP0039/2010; J.F. Schneider: FAPESP grant 2011/18271-5; A.A. Negreti: CAPES fellowship; C.L. Yano: FAPESP fellowship 2010/10674-0; M.H. Krieger: FAPESP grant 2011/07376-0 and CNPq fellowship. The authors also thank M.Sc. Jose Humberto Lopes and the laboratory of the 3M Brasil production plant at Ribeirão Preto, SP, for adhesion tests of coatings and DEGUSSA for GLYMO samples.

References

- Hanawa, T. *Sci. Technol. Adv. Mater.* **2012**, *13*, 064102. doi:10.1088/1468-6996/13/6/064102.
- Vallet-Regi, M.; Colilla, M.; Gonzalez, B. *Chem. Soc. Rev.* **2011**, *40*, 596. doi:10.1039/c0cs00025f.
- Chiriac, A. P.; Neamtu, I.; Nita, L. E.; Nistor, M. T. *Mini-Rev. Med. Chem.* **2010**, *10*, 990. doi:10.2174/1389557511009010990.
- Lendlein, A.; Behl, M.; Hiebl, B.; Wischke, C. *Exp. Rev. Med. Dev.* **2010**, *7*, 357. doi:10.1586/erd.10.8.
- Marrey, R. V.; Burgermeister, R.; Grishaber, R. B.; Ritchie, R. O. *Biomaterials* **2006**, *27*, 1988. doi:10.1016/j.biomaterials.2005.10.012.
- Anderson, J. M. *Annu. Rev. Mat. Res.* **2001**, *31*, 81. doi:10.1146/annurev.matsci.31.1.81.
- O'Brien, B.; Carroll, W. *Acta Biomater.* **2009**, *5*, 945. doi:10.1016/j.actbio.2008.11.012.
- Thierry, B.; Tabrizian, M. *J. Endovasc. Ther.* **2003**, *10*, 807. doi:10.1583/1545-1550(2003)010<0807:BABOME>2.0.CO;2.
- Chaabane, C.; Otsuka, F.; Virmani, R.; Bochaton-Piallat, M. L. *Cardiovasc. Res.* **2013**, *99*, 353. doi:10.1093/cvr/cvt115.
- Kraitzer, A.; Kloog, Y.; Zilberman, M. *J. Biomed. Mater. Res., Part B* **2008**, *85B*, 583. doi:10.1002/jbmb.b.30974.
- Khan, W.; Farah, S.; Domb, A. J. *J. Controlled Release* **2012**, *161*, 703. doi:10.1016/j.jconrel.2012.02.010.
- Puranik, A. S.; Dawson, E. R.; Peppas, N. A. *Int. J. Pharm.* **2013**, *441*, 665. doi:10.1016/j.ijpharm.2012.10.029.
- Thipparaboina, R.; Khan, W.; Domb, A. J. *Int. J. Pharm.* **2013**, *454*, 4. doi:10.1016/j.ijpharm.2013.07.005.
- Gad, S. C. *Standards and Methods for Assessing the Safety and Biocompatibility of Biomaterials*; Jaffe, M.; Hammond, W.; Tolia, P.; Arinzech, T., Eds.; Woodhead Publishing: Sawston, UK, 2013; p. 285.
- Farhatnia, Y.; Tan, A.; Motiwala, A.; Cousins, B.G.; Seifalian, A.M. *Biotechnol. Adv.* **2013**, *31*, 524. doi:10.1016/j.biotechadv.2012.12.010.
- Galli, C.; Coen, M. C.; Hauert, R.; Katanaev, V. L.; Groning, P.; Schlapbach, L. *Colloids Surf. B* **2002**, *26*, 255. doi:10.1016/S0927-7765(02)00015-2.
- Jacobs, T.; Morent, R.; De Geyter, N.; Dubruel, P.; Leys, C. *Plasma Chem. Plasma Process.* **2012**, *32*, 1039. doi:10.1007/s11090-012-9394-8.
- Castner, D. G.; Ratner, B. D. *Surf. Sci.* **2002**, *500*, 28. doi:10.1016/S0039-6028(01)01587-4.
- Jones, C. F.; Grainger, D. W. *Adv. Drug Delivery Rev.* **2009**, *61*, 438. doi:10.1016/j.addr.2009.03.005.
- Brodbeck, W. G.; Shive, M. S.; Colton, E.; Nakayama, Y.; Matsuda, T.; Anderson, J. M. *J. Biomed. Mater. Res.* **2001**, *55*, 661. doi:10.1002/1097-4636(20010615)55:4<661::AID-JBMM1061>3.0.CO;2-F.
- Ciriminna, R.; Fidalgo, A.; Pandarus, V.; Beland, F.; Ilharco, L. M.; Pagliaro, M. *Chem. Rev.* **2013**, *113*, 6592. doi:10.1021/cr300399c.
- Hench, L. L.; West, J. K. *Chem. Rev.* **1990**, *90*, 33. doi:10.1021/cr00099a003.
- Hay, J. N.; Raval, H. M. *Chem. Mater.* **2001**, *13*, 3396. doi:10.1021/cm011024n.
- Galliano, P.; De Damborenea, J. J.; Pascual, M. J.; Duran, A. J. *Sol-Gel Sci. Technol.* **1998**, *13*, 723. doi:10.1023/A:1008653208083.
- Gallardo, J.; Duran, A.; De Damborenea, J. J. *Corros. Sci.* **2004**, *46*, 795. doi:10.1016/S0010-938X(03)00185-9.
- Guglielmi, M. J. *Sol-Gel Sci. Technol.* **1997**, *8*, 443. doi:10.1007/BF02436880.
- Wang, D.; Bierwagen, G. R. *Prog. Org. Coat.* **2009**, *64*, 327. doi:10.1016/j.porgcoat.2008.08.010.
- Metroke, T. L.; Parkhill, R. L.; Knobbe, E. T. *Prog. Org. Coat.* **2001**, *41*, 233. doi:10.1016/S0300-9440(01)00134-5.
- Galvan, J. C.; Saldana, L.; Multigner, M.; Calzado-Martin, A.; Larrea, M.; Serra, C.; Vilaboia, N.; Gonzalez-Carrasco, J. L. *J. Mater. Sci.: Mater. Med.* **2012**, *23*, 657. doi:10.1007/s10856-012-4549-y.
- Wen, J. Y.; Wilkes, G. L. *Chem. Mater.* **1996**, *8*, 1667. doi:10.1021/cm9601143.
- Avnir, D.; Coradin, T.; Lev, O.; Livage, J. *J. Mater. Chem.* **2006**, *16*, 1013. doi:10.1039/B512706H.
- Coradin, T.; Boissiere, M.; Livage, J. *Curr. Med. Chem.* **2006**, *13*, 99. doi:10.2174/092986706789803044.
- Gupta, R.; Kumar, A. *Biomed. Mater.* **2008**, *3*, 034005. doi:10.1088/1748-6041/3/3/034005.
- Bottcher, H.; Slowik, P.; Suss, W. *J. Sol-Gel Sci. Technol.* **1998**, *13*, 277. doi:10.1023/A:1008603622543.
- Asefa, T.; Tao, Z. M. *Can. J. Chem.* **2012**, *90* (12), 1015. doi:10.1139/v2012-094.
- Tsuru, K.; Hayakawa, S.; Osaka, A. *J. Sol-Gel Sci. Technol.* **2004**, *32*, 201. doi:10.1007/s10971-004-5789-1.
- Hetrick, E. M.; Schoenfish, M. H. *Chem. Soc. Rev.* **2006**, *35*, 780. doi:10.1039/b515219b.
- Tfouni, E.; Truzzi, D. R.; Tavares, A.; Gomes, A. J.; Figueiredo, L. E.; Franco, D. W. *Nitric Oxide* **2012**, *26*, 38. doi:10.1016/j.niox.2011.11.005.
- Tfouni, E.; Doro, F. G.; Gomes, A. J.; da Silva, R. S.; Metzker, G.; Benini, P. G. Z.; Franco, D. W. *Coord. Chem. Rev.* **2010**, *254*, 355. doi:10.1016/j.ccr.2009.10.011.
- Brinker, C. J. *J. Non-Cryst. Solids* **1988**, *100*, 31. doi:10.1016/0022-3093(88)90005-1.
- Owens, D. K.; Wendt, R. C. *J. Appl. Polym. Sci.* **1969**, *13*, 1741. doi:10.1002/app.1969.070130815.
- American Society for Test and Materials. *Standard Test Methods for 707 Peel Strength of Adhesive Bonds*; Designation D-1000; American Society for Testing and Materials, West Conshohocken, PA, 2007.
- Buonassisi, V.; Venter, J. C. *Proc. Natl. Acad. Sci. U.S.A.* **1976**, *73*, 1612. doi:10.1073/pnas.73.5.1612.
- Janiszewski, M.; Lopes, L. R.; Carmo, A. O.; Pedro, M. A.; Brandes, R. P.; Santos, C. X. C.; Laurindo, F. R. M. *J. Biol. Chem.* **2005**, *280*, 40813. doi:10.1074/jbc.M509255200.
- Mosmann, T. *J. Immunol. Methods* **1983**, *65*, 55.
- Morshed, M. M.; McNamara, B. P.; Cameron, D. C.; Hashmi, M. S. J. *Surf. Coat. Technol.* **2003**, *163*, 541. doi:10.1016/0022-1759(83)90303-4.
- Jeong, Y. K.; Kim, H. I.; Kim, S. S.; Chung, K. H.; Jang, Y. S.; Park, K. D. *J. Controlled Release* **2003**, *92*, 83. doi:10.1016/S0168-3659(03)00305-5.
- Meth, S.; Sukenik, C. N. *Thin Solid Films* **2003**, *425*, 49. doi:10.1016/S0040-6090(02)01296-8.
- Metroke, T. L.; Kachurina, O.; Knobbe, E. T. *Prog. Org. Coat.* **2002**, *44*, 295. doi:10.1016/S0300-9440(02)00063-2.
- Yabuta, T.; Tsuru, K.; Hayakawa, S.; Osaka, A. *J. Sol-Gel Sci. Technol.* **2004**, *31*, 273. doi:10.1023/B:JSST.0000048002.65187.3a.
- Richards, R. E.; Thompson, H. W. *J. Chem. Soc.* **1949**, *124*. doi:10.1039/JR9490000124.
- Chazalviel, J. N.; Rodrigues, U. P. *Thin Solid Films* **2012**, *520*, 3918. doi:10.1016/j.tsf.2012.01.046.
- Velasco, M. J.; Rubio, J.; Oteo, J. L. *Bol. Soc. Esp. Ceram. Vidrio* **2001**, *40*, 37. doi:10.3989/cyv.2001.v40.i1.760.
- Innocenzi, P.; Brusatin, G.; Guglielmi, M.; Bertani, R. *Chem. Mater.* **1999**, *11*, 1672. doi:10.1021/cm980734z.
- Yim, H.; Kent, M. S.; Tallant, D. R.; Garcia, M. J.; Majewski, J. *Langmuir* **2005**, *21*, 4382. doi:10.1021/la0474870.
- Peeters, M. P. J.; Wakelkamp, W. J. J.; Kentgens, A. P. M. *J. Non-Cryst. Solids* **1995**, *189*, 77. doi:10.1016/0022-3093(95)00248-0.
- Harris, R. K.; Kennedy, J. D.; McFarlane, W. *NMR and the Periodic Table*; Academic Press: London, UK, 1978.
- Engelhardt, G.; Michel, D. *High-Resolution Solid-State NMR of Silicates and Zeolites*; John Wiley & Sons: Chichester, UK, 1987.
- Komori, Y.; Nakashima, H.; Hayashi, S.; Sugahara, Y. *J. Non-Cryst. Solids* **2005**, *351*, 97. doi:10.1016/j.jnoncrsol.2004.10.005.
- Templin, M.; Wiesner, U.; Spiess, H. W. *Adv. Mater.* **1997**, *9*, 814. doi:10.1002/adma.19970091011.
- Uilk, J.; Bullock, S.; Johnston, E.; Myers, S. A.; Merwin, L.; Wynne, K. J. *Macromolecules* **2000**, *33*, 8791. doi:10.1021/ma000023y.
- Fitton, J. H.; Dalton, B. A.; Beumer, G.; Johnson, G.; Griesser, H. J.; Steele, J. G. *J. Biomed. Mater. Res.* **1998**, *42*, 245. doi:10.1002/(SICI)1097-4636(199811)42:2<245::AID-JBM9>3.0.CO;2-2.
- Lee, J. N.; Jiang, X.; Ryan, D.; Whitesides, G. M. *Langmuir* **2004**, *20*, 11684. doi:10.1021/la048562+.
- Yildirim, A.; Budunoglu, H.; Deniz, H.; Guler, M. O.; Bayindir, M. *Appl. Mater. Interfaces* **2010**, *2*, 2892. doi:10.1021/am100568c.
- Zhang, G.; Fu, N.; Zhang, H.; Wang, J. Y.; Hou, X. L.; Yang, B.; Shen, J. C.; Li, Y. S.; Jiang, L. *Langmuir* **2003**, *19*, 2434. doi:10.1021/la025695r.
- Steele, J. G.; Johnson, G.; Mclean, K. M.; Beumer, G. J.; Griesser, H. J. *J. Biomed. Mater. Res.* **2000**, *50*, 475. doi:10.1002/(SICI)1097-4636(20000615)50:4<475::AID-JBM2>3.0.CO;2-G.
- Ceyhan, T.; Tatlier, M.; Akcakaya, H. *J. Mater. Sci.: Mater. Med.* **2007**, *18*, 1557. doi:10.1007/s10856-007-3049-y.
- Dave, B. C.; Hu, X. K.; Devaraj, Y.; Dhali, S. K. *J. Sol-Gel Sci. Technol.* **2004**, *32*, 143. doi:10.1007/s10971-004-5779-3.
- Veranth, J. M. *In Vitro Models for Nanoparticle Toxicology*; In *Nanoscience and Nanotechnology: Environmental and Health Impacts*; Grassian, V. H., Eds.; John Wiley & Sons: Hoboken, NJ, 2008; p. 261.
- Liu, X.; Sun, J. A. *Biomaterials* **2010**, *31*, 8198. doi:10.1016/j.biomaterials.2010.07.069.
- Ma, Z. W.; Mao, Z. W.; Gao, C. Y. *Colloids Surf. B* **2007**, *60*, 137. doi:10.1016/j.colsurfb.2007.06.019.